◆ Human Brain Mapping 28:263–274 (2007) ◆

Hemodynamic Responses in Neural Circuitries for Detection of Visual Target and Novelty: An Event-Related fMRI Study

Ruben C. Gur,[1,2*] Bruce I. Turetsky,[1] James Loughead,[1] Jonathan Waxman,[1] Wendy Snyder,[1] J. Daniel Ragland,[1] Mark A. Elliott,[2] Warren B. Bilker,[1,3] Steven E. Arnold,[1] and Raquel E. Gur[1,2]

[1]*Department of Psychiatry, University of Pennsylvania Medical Center, Philadelphia, Pennsylvania*
[2]*Department of Radiology, University of Pennsylvania Medical Center, Philadelphia, Pennsylvania*
[3]*Department of Biostatistics, University of Pennsylvania Medical Center, Philadelphia, Pennsylvania*

Abstract: The oddball paradigm examines attentional processes by establishing neural substrates for target detection and novelty. Event-related functional imaging enables characterization of hemodynamic changes associated with these processes. We studied 36 healthy participants (17 men) applying a visual oddball event-related design at 4 Tesla, and performed an unbiased determination of the hemodynamic response function (HRF). Targets were associated with bilateral, albeit leftward predominant changes in frontal-parietal temporal and occipital cortices, and limbic and basal ganglia regions. Activation to novelty was more posteriorly distributed, and frontal activation occurred only on the right, while robust activation was seen in occipital regions bilaterally. Overlapping regions were left thalamus, caudate and cuneus and right parietal precuneus. While robust HRFs characterized most regions, target detection was associated with a negative HRF in the right parietal precuneus and a biphasic HRF in thalamus, basal ganglia, and all occipital regions. Both height of the HRF and longer time to peak in the right cingulate were associated with slower response time. Sex differences were observed, with higher HRF peaks for novelty in men in right occipital regions, and longer time to peak in the left hemisphere. Age was associated with reduced peak HRF in left frontal region. Thus, indices of the HRF can be used to better understand the relationship between hemodynamic changes and performance and can be sensitive to individual differences. *Hum Brain Mapp 28:263–274, 2007.*

Key words: HRF; oddball; attention; visual ERP; cerebral activity

INTRODUCTION

Attention requires the complementary processes of directed behavior (top-down control) and response to irrelevant but intrusive novel stimuli that may occur during task performance (bottom-up). These attentional systems have been studied using the oddball paradigm with electroencephalography to measure event-related potentials (EEG-ERPs), elicited by infrequent (target) stimuli interspersed with novel (distractor) stimuli (Knight and Nakada, 1998; Sutton et al., 1965). The associated P300 responses have distinct temporal characteristics, with responses to targets (P3b; Picton, 1992) being delayed relative to responses to novelty (P3a; Courchesne et al., 1975; Friedman et al.,

Ruben served as Consultant to Current Design, Philadelphia, PA, which manufactured the fiber-optic response panel (FORP) used in the study.

Contract grant sponsor: National Institute of Health; Contract grant numbers: MH-64045, MH-19112, and M01RR0040.

*Correspondence to: Dr. Ruben C. Gur, Brain Behavior Laboratory, 10th Floor Gates Pavilion, University of Pennsylvania Medical Center, Philadelphia, PA 19104. E-mail: gur@bbl.med.upenn.edu

Received for publication 15 August 2004; Revised 29 November 2004; Accepted 15 December 2004

DOI: 10.1002/hbm.20319

Published online 28 November 2006 in Wiley InterScience (www.interscience.wiley.com).

1998; Squires et al., 1975). The P3a response is conceptualized as a cognitive "orienting" to unexpected stimuli (Courchesne, 1978; Courchesne et al., 1975). The P3b, in contrast, is thought to reflect processes related to working memory (Donchin, 1981). The EEG-ERP data also suggest a different topography for these systems, with the novelty response showing both a more posterior parietal distribution and an anterior component (Goldstein et al., 2002; Spencer et al., 2001). Such ERP measures have been related to individual differences in healthy people (e.g., Hirayasu et al., 2000; Hoffman and Polich, 1999; Maeshima et al., 2003) and clinical populations (e.g., Ford et al., 2004; Knight and Nakada, 1998). An investigation of patients with frontal lesions indicated that orienting to novel stimuli appears to be mediated through dorsal prefrontal cortex, though this may not be the actual site of the neural generators of the P3a (Knight, 1984). Such data have also suggested that the response to task-salient stimuli is critically dependent upon the area of the temporal parietal junction and inferior parietal lobule (Knight et al., 1988).

While EEG-ERP studies provide precise timing of the brain's response to targets and novel distractors, the "inverse problem" constrains topographic characterizations of distributed neural systems (e.g., Hori et al., 2004). Event-related fMRI provides spatial resolution that can be exploited by administering oddball procedures with established EEG-ERP effects. Studies with fMRI have examined change in the blood oxygenation level dependent (BOLD) signal for visual targets and novel distractors relative to non-targets. While EEG-ERP studies have commonly applied auditory paradigms, most fMRI-ERP studies have included the visual modality. McCarthy et al. (1997) demonstrated evoked changes for visual targets in the middle frontal gyrus in excess of activation to novel stimuli (Kirino et al., 2000). Other studies have examined the entire brain for voxels that show changes consistent with a hemodynamic response ("biased analysis") to targets and novels. Target presentations were associated with activations resembling a hemodynamic response in a distributed system that included supramarginal gyrus, frontal, insula, thalamus, cerebellum, occipital-temporal, superior temporal, and cingulate regions (Ardekani et al., 2002; Clark et al., 2000; Huettel and McCarthy, 2004; Linden et al., 1999). Presentation of distractors evoked activation of a distinct system, which included anterior cingulate, frontal, inferior parietal, occipital, and temporal regions (Clark et al., 2000).

These fMRI studies have helped characterize the neural networks for target detection and distractor or novelty processing. Corbetta and Shulman (2002) proposed that the target detection system includes parietal and superior frontal cortex while the bottom-up system evoked by salient distractors is more ventral and includes temporoparietal and inferior frontal cortex. This hypothesis received some support. Bledowski et al. (2004) used a three-stimulus visual ERP paradigm in a biased analysis and found partially overlapping but distinguishable systems for target detection and response to repeated distractors matched for complexity. However, the distractors were neither novel nor salient, as all stimuli were either circles or squares. Kiehl and Liddle (2003) applied the auditory oddball paradigm with standard, target, and novel (complex non-repeating sounds) stimuli, and documented repeatable activations consistent with hemodynamic responses to target in frontal, temporal, parietal, cerebellar, and subcortical regions. Novel stimuli elicited activation in lateral frontal and temporal areas and in inferior parietal cortex. There is convergence between the visual and auditory systems in response to targets, while distractors elicit responses in the respective sensory regions. The main purpose of the present study was to test this hypothesis using tasks that are exact reproductions, within the fMRI scanning environment, of conditions that have been studied extensively with EEG-ERP.

In addition to testing the hypothesis, we examined the utility of an "unbiased analyses" of fMRI BOLD changes (Hulvershorn et al., 2005). In this analysis no predetermined HRF is assumed. Except for studies that have delineated specific predetermined regions of interest (Bledowski et al., 2004; Kirino et al., 2000; McCarthy et al., 1997), analyses to date have used a "biased" search for regions that show changes conforming to a predetermined canonical HRF. Our approach enables an evaluation of inter-regional and individual differences in HRF characteristics, which can inform about mechanisms and functional relations between brain activation and behavior. Our study was sufficiently powered to examine relations between performance and HRF parameters. Such associations can help interpret the functional significance of task-related hemodynamic changes (Gur et al., 1992). The sample also enabled evaluation of sex differences and age effects on the HRF parameters. Both gender and age are important moderating variables affecting cerebral blood flow (CBF) (Gur et al., 1982, 1987, 2000; Madden et al., 2004; Shaywitz et al., 1995) and EEG-ERP measures (Bahramali et al., 1999; Coyle et al., 1991; Fjell and Walhovd, 2003; Hirayasu et al., 2000; Hoffman and Polich, 1999).

MATERIALS AND METHODS

Participants

The sample included 36 healthy adults (17 men, 19 women) who were consecutive right-handed volunteers at the Brain Behavior Laboratory of the University of Pennsylvania. Mean age ± SD was 30.1 ± 8.3 years (range 18–48) and education 16.0 ± 2.8 years (range 10–20). Three additional subjects (2 men, 1 woman) were excluded after inspection of fMRI data revealed greater than 4 mm translational motion in any direction. Participants underwent standardized screening and evaluation procedures, consisting of medical, neurological, psychiatric (SCID-NP, First et al., 1995) examinations, and laboratory tests. They had no history of illness affecting brain function or major psychiatric illness in first-degree relatives and were not taking any medication. The study was conducted in compliance with

the Code of Ethics of the World Medical Association (Declaration of Helsinki) and the standards established by the University of Pennsylvania Institutional Review Board and the National Institute of Health. After complete description of the study, written informed consent was obtained.

Experimental Tasks

Three stimulus types were presented in a random order: standards, targets, and novels (Fig. 1). The standard frequent stimulus was a circular arrangement of small bright red Gabor elements (red circle) set against a gray textured background with randomly distributed light-gray Gabor elements. The target infrequent stimulus, a green circle, differed only in color. The novel stimuli were fractal images created with commercial software (ArtMatic v1.2.1, U&I Software, 1999). Luminance of the novel stimuli was the same as that of the target and standard. A total of 200 stimuli were presented, with 15% targets, 15% novels, and 70% standards. They followed 10 filler stimuli (9 standard, 1 target) presented prior to usable image acquisition. Each stimulus was presented for 1 sec, with a 1 sec inter-stimulus interval during which a homogeneous visual noise gray background was displayed. Responses and reaction times to all stimuli were recorded. The test required 400 sec to complete.

Procedures

Participants completed a practice task containing no novel stimuli before being placed in the scanner. Earplugs were fitted to muffle scanner noise and head fixation was assured through a foam-rubber device mounted on the head coil. Stimuli rear projected onto a screen that participants viewed through a mirror mounted inside the gantry.

The scanner synchronized task administration with image acquisition through the PowerLaboratoryÿ platform (Chute and Westall, 1997) on a Macintosh Powerbook computer. After random assignment of response hand, the participant was instructed to press a single button of a response pad (FORP^{TM}, Current Design, Philadelphia, PA) when the infrequent target stimulus appeared. They were not told that novel stimuli would also be shown. No response was required for the standard or novel stimuli to simplify the response component and make the study more comparable to standard auditory ERP procedures (e.g., Bledowski et al., 2004).

fMRI Data Acquisition

Data were acquired using blood oxygenation-level dependent (BOLD) contrasts in a 4T GE Signa Scanner (Milwaukee, WI), employing a quadrature head coil. Structural images consisted of a sagittal T1-weighted localizer, followed by a T1-weighted acquisition of the entire brain in the axial plane (24 cm FOV, 256 × 256 matrix, resulting in voxel size of 0.9375 × 0.9375 × 4 mm^3). This sequence was used for spatial normalization to a standard atlas (Talairach and Tournoux, 1988) and for anatomic overlays of the functional data. Functional imaging was performed in the axial plane using multislice gradient-echo echo planar imaging with a field of view of 24 cm (frequency) × 15 cm (phase), and an acquisition matrix of 64 × 40 (22 slices, 4 mm thickness, 0 slice gap, TR = 2,000 ms, TE = 21 ms). The 22 slices were acquired from the superior cerebellum up through the frontal lobe. Inferiorly this corresponded to a level just below the inferior aspect of the temporal lobes. Superiorly this corresponded to approximately the level of the hand-motor area in the primary motor cortex. This sequence delivered a nominal voxel resolution of 3.75 × 3.75 × 4 mm^3.

Image Analysis

Functional images were preprocessed in MEDx^{TM} using standard procedures (Ragland et al., 2002). Images were motion corrected (Woods et al., 1993), proportionally scaled (Andersson, 1997), and filtered using a bandpass Butterworth filter (6–60 s; Friston et al., 2000). Talairach transformation (Talairach and Tournoux, 1988) occurred in two steps. First, a least-squares surface registration algorithm (Pelizzari et al., 1989) coregistered raw functional images to the structural localizer. Second, a nonlinear transformation into Talairach space was based on commissural landmarks identified by a trained investigator. Transformed data were spatially smoothed (8 mm FWHM, isotropic). Finally, a conjoined activity mask was created by thresholding each image in a subject's time-series at 10% of the mean of the maximum for all images.

A multi-subject analysis was performed using a two-stage random-effects approach. Individual fMRI time series data were regressed to three general linear models specifying predictor variables for (1) the target stimuli only (target model), (2) the novel stimuli only (novel model), and (3) both target and novel stimuli (full model). The unbiased hemodynamic responses to the target and novel stimuli were determined for each model using a previously described method (Hulvershorn et al., 2005), which does not rely on an assumed canonical response function. This method of analysis is equivalent to a deconvolution of the HRF from the stimulus-timing vector (Dale, 1999).

This analysis relies on the assumptions that the hemodynamic response sums linearly over trials (Boynton et al., 1996) and is negligible after 16 sec (Kruggel and von Cramon, 1999; Liu et al., 2000). These assumptions are supported for interstimulus intervals of 1,000 msec or greater (Rosen et al., 1998). The resulting unbiased HRF parameters (beta amplitudes) correspond to estimates of the hemodynamic response at ten time points (i.e., TR periods), beginning 4 sec prior to the stimulus onset and ending 14 sec after the onset. The HRF beta amplitudes were converted to percent change from baseline and then baseline corrected to the mean of the two prestimulus time points.

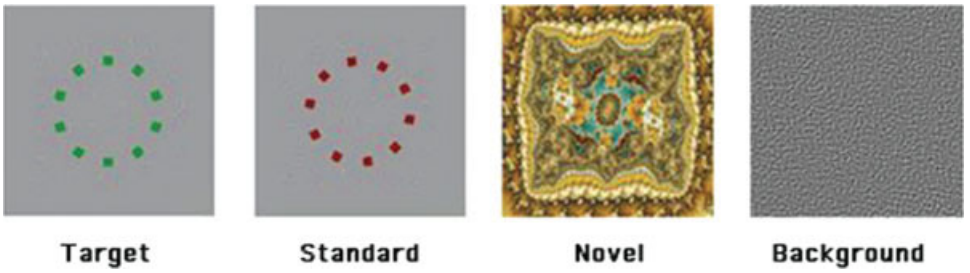

Figure 1.
Illustration of the standard, target, and novel stimuli.

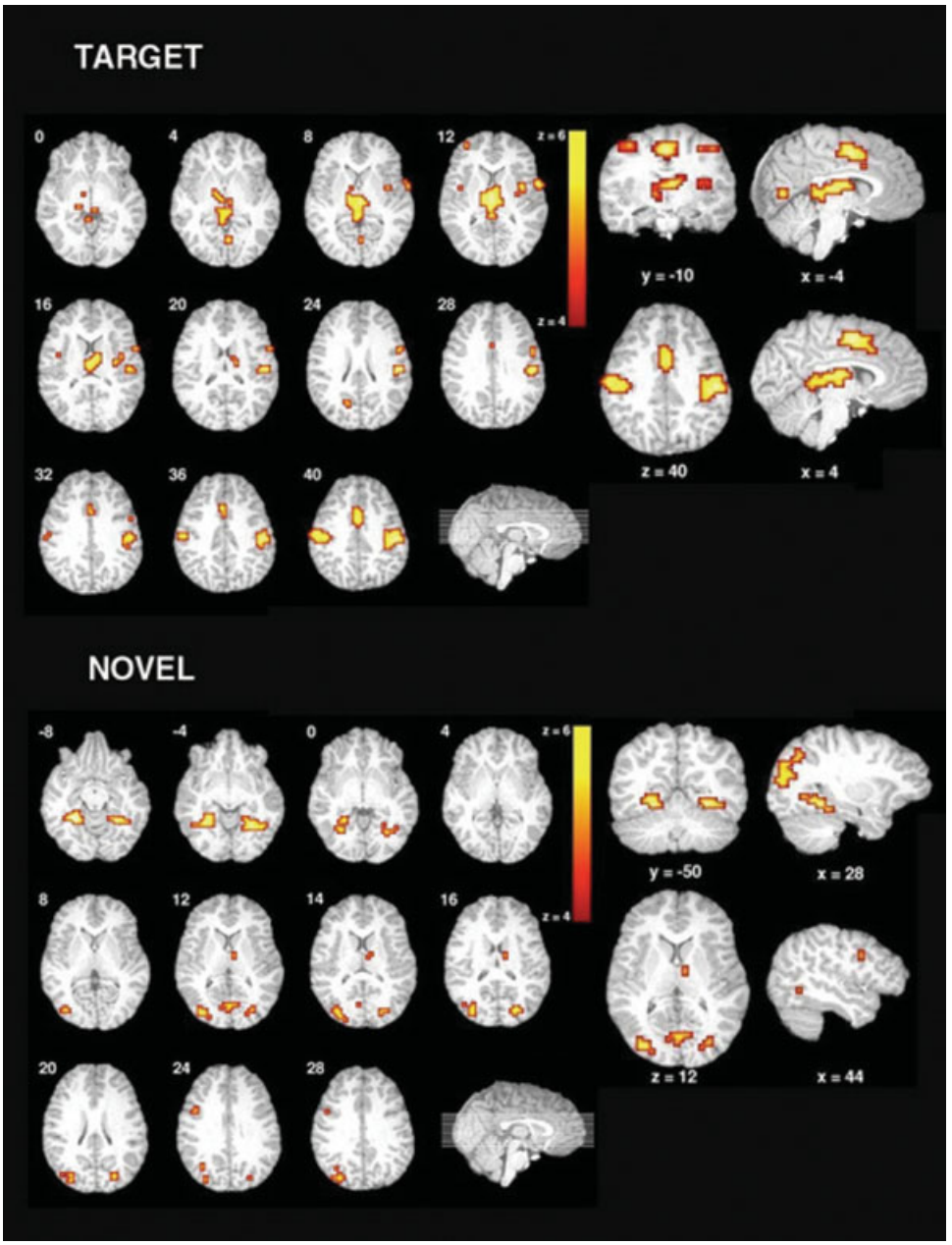

Figure 2.
Activation maps for the target (upper display) and novel (bottom display) conditions. Brain images showing the partial *Z* map are displayed in radiological convention (left is to the viewer's right). Colored areas exceed a corrected *P* value of 0.05.

Each model regression produced an R^2 value for every voxel timecourse in the functional image data. The R^2 results from the target and novel models were converted to partial F statistics utilizing the expression

$$F_{\text{target}} = \frac{\frac{R^2_{\text{full}} - R^2_{\text{target}}}{M_{\text{target}}}}{\frac{1 - R^2_{\text{full}}}{N - M_{\text{target}} - M_{\text{novel}} - 1}} \quad (1)$$

and

$$F_{\text{novel}} = \frac{\frac{R^2_{\text{full}} - R^2_{\text{novel}}}{M_{\text{novel}}}}{\frac{1 - R^2_{\text{full}}}{N - M_{\text{novel}} - M_{\text{target}} - 1}}, \quad (2)$$

where M_{target} and M_{novel} are the number of vectors regressed in the target and novel models, respectively. These results produced partial F maps subsequently converted to Z maps via corresponding P values. Group activation maps for target and novel conditions were generated by entering individual partial Z maps into separate single group t tests. Final significance thresholds were based on spatial extent (k) and peak height (u) (Forman et al., 1995) resulting in corrected probability of $P \leq 0.05$, based on the theory of Gaussian fields (Friston et al., 1994a,b). Identified clusters were sub-divided into anatomical regions using the Talairach Daemon database (Lancaster et al., 1997).

Statistical Analysis

Quantitative analyses were performed on the scaled beta weights reflecting the estimated HRF for the target and the novel contrasts as detailed above. To obtain temporal resolution finer than the TR period, each unbiased HRF was spline-interpolated to a resolution of 10 ms. Four parameters were calculated for each HRF: Max = peak activation, TTP = time to peak activation (in sec), AUCpos = area under the curve above baseline, and AUCneg = area under the curve below baseline. These parameters were calculated for each anatomical region identified in the cluster analysis and subjected to sex × region × hemisphere GEE (generalized estimating equations). GEE was preferred over MANOVA because it accommodates incomplete designs (not all regions were activated bilaterally) and is robust against violations of the sphericity assumption.

To examine the relation between activation and performance, regression analyses were performed separately for each index (MAX, TTP, AUCpos, AUCneg) predicting performance from regional values. Since there was little variability in number of correct target identification, response time (RT in msec) was used as a measure of performance. Associations between HRF indices and age were examined with Pearson correlations.

RESULTS

Activation Maps

The images displaying BOLD changes unique to target appearance are shown in Figure 2 (top). As can be seen, several regions were activated, especially bilateral thalamus, frontal (paracentral, cingulate, medial), parietal (right precuneus, bilateral inferior), and temporo-limbic (superior temporal, cingulate, insula). More restricted changes were evident in left midbrain, caudate, and occipital regions. The activated voxels and their regional peaks are presented in Table I (top). The images showing change unique to appearance of the novel stimuli are presented in Figure 2 (bottom). The main activations were in posterior cortices and included visual, parietal and posterior parahippocampal association areas. More restricted activations were observed in left thalamus and caudate and right midtemporal and inferior frontal cortices. The activated voxels and their regional peaks are presented in Table I (bottom).

Inspection of the HRFs for activated regions (Fig. 3) showed characteristic BOLD signal changes for most regions. The notable exceptions for target were a negative HRF in the right parietal precuneus (second row, second panel from left), and basal ganglia and occipital HRFs showed biphasic (positive followed by negative) excursions. For novel, minimal basal ganglia changes resembling an HRF were seen, even though the overall activation for these regions was significant.

HRF Parameters

Figure 4 illustrates regional changes in the BOLD signal as reflected in each of the HRF parameters. As can be seen, the pattern of HRF parameters shows higher peaks in frontal than in posterior regions for the target contrast but about equal times to peak across regions. For the novel contrast, occipital regions and parahippocampus showed higher peaks relative to frontal, temporal or thalamic regions, again with little regional variability in time to peak. Men and women showed nearly identical patterns, supporting the reproducibility of regional variation in these values. However, some regions and indices appeared to show sex differences, justifying omnibus statistical tests to establish significance of these deviations from the common profile (see below).

Association With Performance

In this sample of healthy volunteers, the range of errors (0–3) was too limited to be used as a dependent measure in a regression analysis. Response time showed sufficient variability (mean ± SD = 480.6 ± 84.8 msec), with no significant difference between men (488.8 ± 67.6, range 382.0–579.0 msec) and women (473.4 ± 99.1, range 343.0–749.0 msec), $t = 0.51$, df = 33, $P = 0.616$, not significant. When response time (RT) was entered as the dependent measure, it was significantly predicted from the MAX of the right cingulate gyrus ($F = 4.37$, df = 1.32, $R^2 = 0.123$, $P = 0.0450$), the TTP of

TABLE I. Mean cluster[a] locations[b] and local maxima[c] of BOLD signal change

	Size	Region (Brodmann area)	x	y	z	P ($n_{max} \geq k$)	Sub-region (Brodmann area)	HEM	Peak Z	x	y	z
Cluster Centroids for Target							Target atlas derived subdivision					
1.	163	Left parietal lobe (2)	−44	−24	40	0.0000	Precentral gyrus (3)	L	4.95	−52	−18	36
							Postcentral gyrus(40)	L	5.88	−44	−30	48
							Inferior parietal (40)	L	5.47	−44	−30	44
2.	129	Left thalamus	−2	−22	10	0.0000	Thalamus	L	5.34	−4	−22	8
							Thalamus	R	5.15	4	−18	12
							Brainstem	L	4.28	−4	−30	0
							Caudate	L	4.40	−12	−2	16
3.	127	Right parietal lobe (4)	44	−22	46	0.0000	Inferior parietal (40)	R	4.57	52	−26	44
							Postcentral gyrus (1)	R	5.39	56	−18	44
							Precentral gyrus (4)	R	5.13	36	−18	52
4.	100	Left limbic lobe (24)	−2	0	44	0.0000	Medial frontal gyrus(6)	L	5.98	−2	−2	48
							Medial frontal gyrus (6)	R	5.53	4	−2	48
							Cingulate gyrus (24)	L	6.06	−2	−2	44
							Cingulate gyrus (24)	R	5.39	4	−2	44
5.	20	Left frontal lobe (6)	−58	4	18	0.0000	Inferior frontal gyrus (9)	L	4.94	−52	2	24
							Precentral gyrus (6)	L	4.84	−52	2	28
							Superior temporal gyrus (22)	L	4.35	−64	−2	8
6.	13	Left insula (13)	−36	−4	12	0.0000	Insula (13)	L	5.00	−32	−10	16
							Claustrum	L	4.09	−32	−10	12
7.	6	Left occipital lobe (18)	−6	−68	6	0.0018	Lingual gyrus (18)	L	4.59	−4	−66	4
							Cuneus (30)	L	4.27	−4	−66	8
8.	3	Right occipital lobe (31)	14	−64	24	0.0169	Precuneus (7)	R	4.21	16	−62	24
9.	3	Left parietal lobe (7)	−26	−60	48	0.0169	Precuneus (7)	L	4.11	−24	−58	48
							Superior parietal (7)	L	4.30	−28	−58	48
10.	2	Right frontal lobe (10)	32	52	12	0.0411	Middle frontal gyrus (10)	R	4.32	32	50	12
11.	2	Right insula (13)	40	−2	14	0.0411	Insula (13)	R	4.38	40	−2	16
Cluster centroids for novel							Novel atlas derived subdivision					
1.	55	Right occipital lobe (19)	30	−74	24	0.0000	Cuneus (19)	R	4.81	28	−78	32
							Middle occipital gyrus(19)	R	5.43	32	−82	12
							Precuneus (7)	R	4.50	28	−66	36
2.	47	Right limbic lobe (37)	26	−48	−6	0.0000	Parahippocampal gyrus (37)	R	6.45	24	−46	−8
							Lingual gyrus (19)	R	4.42	24	−62	0
3.	37	Left limbic lobe (37)	−32	−54	−4	0.0000	Parahippocampal gyrus (37)	L	5.59	−28	−46	−8
							Fusiform gyrus (37)	L	6.25	−28	−50	−8
4.	20	Left occipital lobe (19)	−26	−78	18	0.0000	Cuneus (18)	L	5.03	−24	−78	20
							Middle occipital gyrus (18)	L	5.45	−24	−82	20
5.	10	Left occipital lobe (18)	−2	−72	12	0.0000	Cuneus (18)	R	4.10	8	−74	12
							Cuneus (18)	L	4.11	−8	−70	12
6.	6	Left thalamus	−10	−8	16	0.0012	Thalamus	L	4.22	−8	−6	12
7.	4	Right frontal lobe (9)	42	8	30	0.0058	Inferior frontal gyrus (9)	R	4.22	44	6	32
8.	2	Right temporal lobe (39)	40	−72	22	0.0363	Middle temporal gyrus (39)	R	4.22	40	−70	20

HEM, cerebral hemisphere.
[a] Cluster threshold $Z \geq 4.05$ and corrected P-value < 0.05.
[b] Estimated Brodmann's areas and coordinates from Talairach and Tournoux (1988).
[c] Z values represent peak activation for atlas derived subdivision with greater than two voxels.

that region ($F = 8.20$, df $= 1.32$, $R^2 = 0.209$, $P = 0.0075$), the AUCpos of that region ($F = 6.27$, df$= 1.32$, $R^2 = 0.168$, $P = 0.0178$), and the AUCneg of the left superior temporal gyrus ($F = 7.56$, df $= 1.32$, $R^2 = 0.196$, $P = 0.0099$). In all these cases, higher values were associated with longer response times. When all four predictors were entered simultaneously, we were able to account for 44% of the variance in performance, $F = 7.49$, df $= 4.32$, $P = 0.0007$.

Sex Differences

The GEE on the peak activation levels for the target contrast showed a sex × region, $\chi^2 = 21.64$, df $= 6$, $P = 0.0014$ and a sex × region × hemisphere interaction, $\chi^2 = 15.41$, df $= 6$, $P = 0.0173$. As can be seen in Figure 4 (upper row, leftmost panel), women had greater peak activation in left inferior frontal and right inferior parietal relative to men, who had higher peak activation in the left mid-frontal and the left cingulate gyrus. For the time to peak measure, there was only a main effect of sex, $\chi^2 = 3.91$, df $= 6$, $P = 0.0481$. As can be seen in Figure 4, men tended to have longer times to peak across regions with the difference reaching significance only for the left inferior parietal and thalamus. For the positive area under the curve, there was a sex × region, $\chi^2 = 17.52$, df $= 6$, $P = 0.0076$, a sex × hemisphere, $\chi^2 = 10.59$, df $= 2$, $P = 0.0050$, and a sex ×

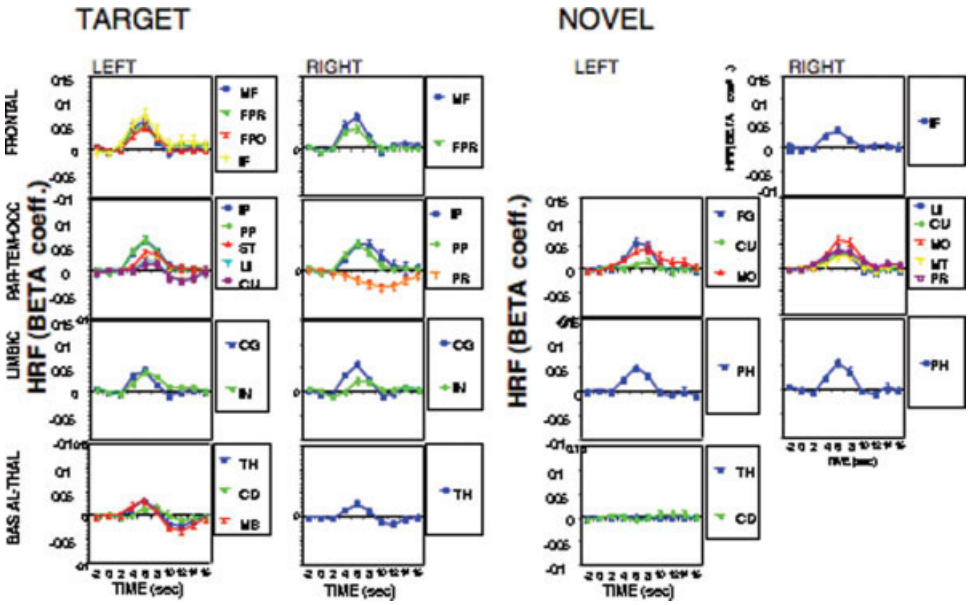

Figure 3.

The HRFs, expressed as percent change in beta coefficients from the regression based estimate of the baseline, in activated regions for the target (left two columns) and novel (right two columns). HRFs are presented separately for frontal (top raw), parietal temporal– occipital (second raw), limbic (third raw), and basal ganglia- thalamic regions (bottom raw). MF = Midfrontal, FPR = Frontal precentral, FPO = Frontal postcentral, IF = Inferior frontal, IP = Inferior parietal, PP = Parietal precuneus, ST = Superior temporal gyrus, LI = Lingual gyrus, CU = Cuneus, CG = Cingulate gyrus, IN = Insula, TH = Thalamus, CD = Caudate, MB = Midbrain, FG = Fusiform gyrus, MO = Mid-occipital, PH = Parahippocampal gyrus, MT = Midtemporal.

region × hemisphere interaction, $\chi^2 = 13.45$, df = 6, $P = 0.0364$. These interactions reflect overall greater positive activation in the left cingulate for men relative to greater left inferior frontal and right inferior parietal for women. For the negative area under the curve, there was a sex × region, $\chi^2 = 18.07$, df = 6, $P = 0.0061$, and a sex × region × hemisphere interaction, $\chi^2 = 16.95$, df = 6, $P = 0.0095$. These interactions reflect more negative HRFs in right hemispheric regions for men than for women, although none of the individual regions showed significant sex differences. The GEE on the peak activation levels for the novel contrast showed only a sex × region interaction, $\chi^2 = 13.28$, df = 1, $P = 0.0389$. As can be seen in Figure 4 (upper row, right panel), men had higher peaks in occipital regions and the parahippocampus bilaterally. No other sex differences or interactions emerged.

Correlations With Age

Increased age showed a small but significant correlation with increased response time, r = 0.332, df = 34, $P = 0.03185$, one-tailed. For target detection, only the left inferior frontal and right insula showed correlations between HRF indices and age. Specifically, for the left inferior frontal region, both peaks and positive area under the curve showed decline with age, $r = -0.360$ and -0.318, df = 34, $P = 0.0167$ and 0.03095, respectively. For the right insula, increased age was associated with a shorter time to peak, a smaller positive area under the curve, and greater negative area under the curve, $r = -0.408$, -0.306, and 0.410, df = 34, $P = 0.0074$, 0.0369, and 0.0072, respectively. For novels, increased age was associated with lower peaks and smaller areas under the curve in the right occipital cuneus, $r = -0.345$ and -0.314, df = 34, $P = 0.0213$ and 0.033, respectively.

DISCUSSION

Our results provide evidence for partially overlapping but separable neural systems for attentional top-down visual target detection and bottom-up novelty processing (Corbetta and Shulman, 2002). Consistent with hypotheses based on EEG-ERP and earlier fMRI-ERP studies, targets were associated with bilateral, albeit leftward predominant changes in frontal-parietal cortex. Signal changes time-locked to target presentation were also observed in temporal and occipital cortices, and limbic and basal ganglia regions. Activation to novelty was more posteriorly distributed, and frontal activation occurred only on the right, while robust activation was seen in occipital regions bilat-

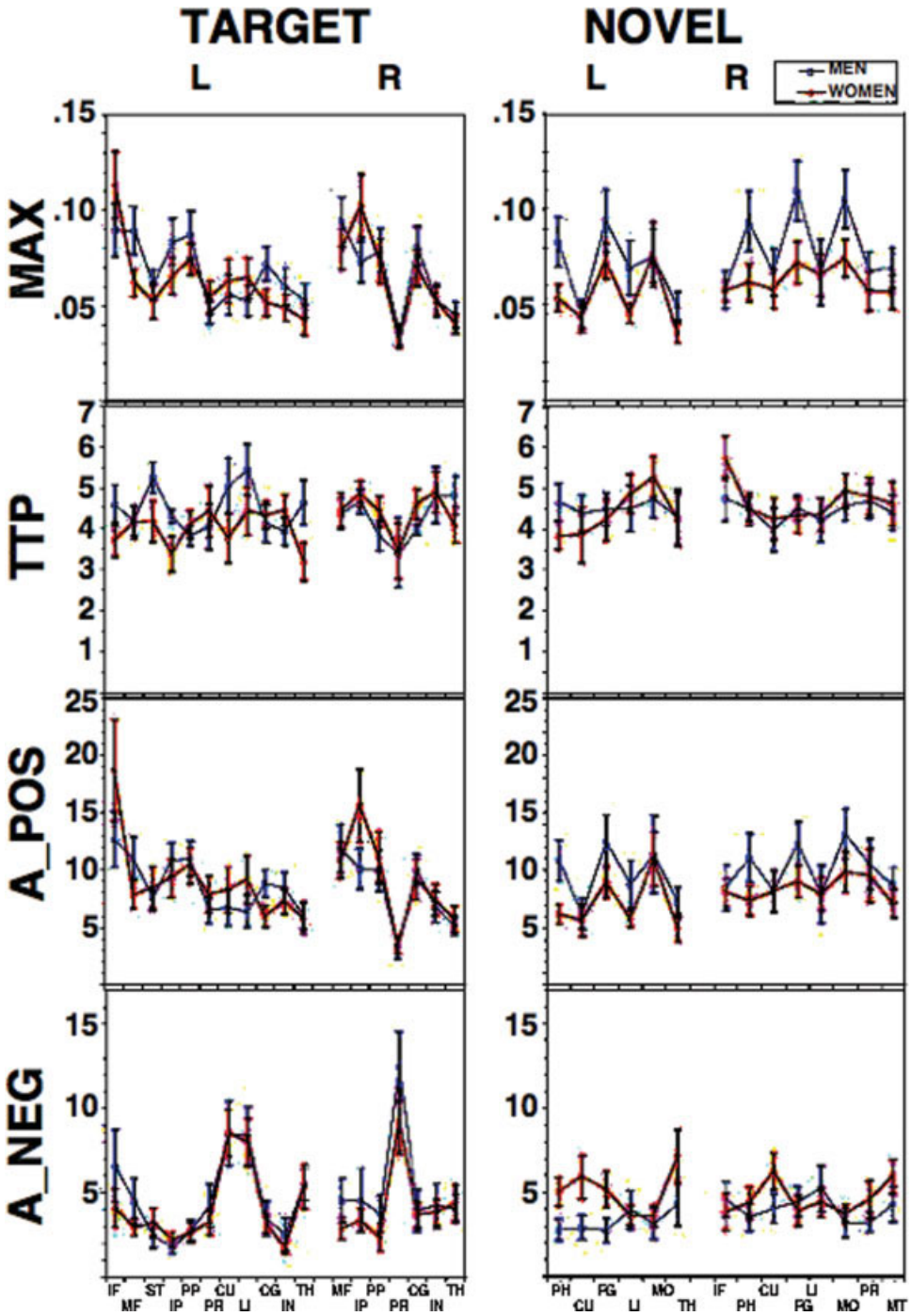

Figure 4.
Indices of the HRF for target (left column) and novel (right column) contrasts. The indices include MAX (top raw), TTF (second raw), AUCpos (third raw), and AUCneg (bottom raw). Region definitions as in Figure 3.

erally. Of the limbic regions, both cingulate and insular cortex showed robust activation for target, but only the parahippocampal gyrus showed bilateral activation for novelty. Areas of convergence for both systems were the left thalamus, caudate and occipital cuneus, and the right parietal precuneus.

These results confirm earlier studies probing the neural substrate of target detection and response to novelty (Ardekani et al., 2002; Bledowski et al., 2004; Clark et al., 2000; Kiehl and Liddle, 2003; Kirino et al., 2000; Knight and Nakada, 1998; Linden et al., 1999; McCarthy et al., 1997). Our unbiased analysis indicated that activation for visual target in primary visual cortex, as well as thalamus and basal ganglia, was of low amplitude and biphasic, and in the right parietal precuneus a robustly negative HRF was observed. By contrast, novel stimuli produced positive

HRFs for all regions showing evoked changes. Indeed, the right precuneus that showed a negative HRF for the target detection had a positive HRF for novel stimuli.

Target stimuli were visually simple and differed from the standard only in the color of the circle, yet they elicited activation of a complex attentional matrix to detect salience and induce decisive action. The network included posterior parietal cortices (inferior parietal and precuneus) for sensory representation, motivational representation in limbic-related cingulate and medial frontal cortices, and pre- and post-central cortices for sensorimotor representation (Mesulam, 1999). Changes observed in reticular brainstem and thalamus likely reflect their role in modulating activation of the network.

The extensive occipital response for novel stimuli was accompanied by bilateral parahippocampal changes, while frontal activation was restricted to its right inferior aspect. These stimuli, while not requiring a decisive response, were visually complex and rich with color, contrast, and contour. They elicited vigorous activation of visual and higher order association areas, possibly reflecting efforts to interpret the complex percepts. The ventromedial activation suggests that our novel stimuli were associated with changes observed as part of the orienting response (Williams et al., 2000).

Analyses of the HRFs suggest that while most followed the classic canonical function, some regions differed. The mild and biphasic activation for targets in the lingual and cuneal occipital areas may reflect the absence of added requirements for visual processing of the target compared to the standard stimuli. Biphasic HRF in thalamus bilaterally and the left caudate and brainstem may relate to their role in salience detection and signaling (Zink et al., 2003). Attention-related midbrain reticular core and thalamic reticular systems are inhibitory on other thalamic nuclei and cortices. The biphasic response may manifest the difference in timing of the thalamic response to target and standard, which may constitute part of the signaling system. This can be tested in designs that include an additional event to which both targets and standards can be contrasted.

Inferences on neuronal activity from the temporal characteristics of the HRF are hindered by the complex interaction of physiologic effects on the BOLD response, including changes in cerebral blood flow, blood volume, and rate of oxygen consumption (Buxton, 2001; Dilharreguy et al., 2003; Duong et al., 2000; Hall et al., 2002; Hulvershorn et al., 2005; Jones et al., 2001; Lee et al., 1995; Vanzetta and Grinvald, 2001; van Zijl et al., 1998). Regional differences in vascular architecture (Robson et al., 1998) can lead to variability in the time evolution of the HRF across the brain (Huettel and McCarthy, 2001; Saad et al., 2001). The negative HRF responses most likely reflect neuronal deactivation and inhibition (Saad et al., 2001; Shmuel et al., 2002). Thus, the negative HRF seen for target in the right precuneus probably indicates reduced activity for target relative to standard.

Evaluation of components of the HRF indicated that the peak of the activation, time to reach peak, as well as the positive and negative areas under the curve, each provide an index that is sensitive to different regional effects and individual differences. The peak of the HRF shows the greatest variability among regions and between the hemispheres. It also shows sex differences for the novel contrast, men had higher peaks in the parahippocampal gyrus bilaterally and the right fusiform and mid-occipital regions. The greater activation in men for novelty is consistent with EEG-ERP studies in humans (Nagy et al., 2003) and with evidence from rodents that males have greater behavioral response to novel spatial stimuli (e.g., Frick and Gresack, 2003). Time to peak showed the least amount of inter-regional variability, averaging about 4 sec after stimulus onset, and while overall it was longer for men for the target contrast in the left hemisphere, this difference approached significance only for superior temporal gyrus, inferior parietal lobule, and thalamus. The positive area under the curve showed effects similar to those seen for peak, while the negative area under the curve was particularly prominent in the left occipital, and right percuneus. Notably, we examined sex differences because of their impact on CBF (Gur et al., 1982, 2000; Madden et al., 2004; Shaywitz et al., 1995) and ERP-EEG (Hirayasu et al., 2000; Hoffman and Polich, 1999), but the tasks were not selected for showing sex differences and indeed none were found in performance. The sex differences we observed are therefore subtle, but may explain downstream effects in studies where such differences in performance are prominent. For example, the enhanced response to novel distractors in men could relate to their greater susceptibility to attention deficit disorder. These effects encourage further investigation of both the spatial and time course characteristics of the HRF in men and women.

Some insight on the significance of the HRF characteristics can be gleaned from correlating HRF indices with performance. The right cingulate gyrus yielded activation parameters most predictive of performance. This is consistent with evidence for its role in conflict resolution and response modulation (Kerns et al., 2004). Congruent with the notion that a stronger hemodynamic response reflects greater effort (e.g., Gur et al., 1997), higher HRF amplitude with longer time to peak predicted longer response latency. That the effect was predominantly in the right cingulate may reflect its increased activation for individuals who had greater difficulty in this go-no-go conflict resolution. In contrast to activation measures, quantitative indices of overall rates of CBF have consistently shown positive correlations with performance (Gur et al., 1997). While BOLD fMRI studies do not provide a measure of CBF rate, but only changes sensitive to oxygenation level, methods for quantitative measurement of CBF with fMRI are available (Wang et al., 2003). These could be used to examine both basal CBF levels and task-related activation. Interpreting the association between performance and negative area under the curve for the left superior temporal gyrus must

await further clarification of the meaning of this activation index.

The correlations between age and HRF indices were region specific and small. For target detection, both lower peaks and smaller positive areas under the curve in the left inferior frontal region suggested weaker HRFs with increased age. For insula, the shorter time to peak with increased age was associated with reduced positive areas under the curve and increased negative areas under the curve, perhaps reflecting rapid but weaker activation that induces accelerated oxygen depletion. For novelty, increased age was associated with lower peaks and smaller areas under the curve in the right occipital cuneus. While the limited age range in this study of young adults has likely truncated the correlations, they are consistent with regions showing age differences between young and elderly adults in Madden et al.'s (2004) study with visual fMRI-ERP. This consistency supports the potential sensitivity of HRF indices to age effects.

Our study has several limitations. Because a stimulus was presented during each acquisition we were unable to resolve HRFs unique to the standard. Designs incorporating "null event" scans are needed for such determination. With regard to correlating activation with performance, we have used a task that was too easy to generate a reliable index of accuracy and had to rely on response time. The task was made easy to restrict activation to regions uniquely devoted to target detection, without recruitment of complex computational or executive processes, and to permit study of patients with brain dysfunction. More difficult target detection tasks, however, could reveal robust predictors of performance accuracy separable from speed. Such designs could detect regions whose activation is associated with errors, and these regions may constitute the distributed system associated with the error component of the P300 (Gehring et al., 1993). Another limitation of the study is the complexity of the novel stimuli, which may have introduced some confounding of the novelty effects. It is quite possible, for example, that fewer occipital regions will be activated with less complex stimuli. On the other hand, more simple novel non-repeating stimuli will induce habituation. Our complex, non-verbalizable and non-repeated novel distractors more nearly approximate the type of stimuli used in auditory P300 EEG-ERP studies, and arguably provide a better simulation of intrusive percept that may interrupt an attentional task in real life.

CONCLUSIONS

Our study with visual stimuli supported the hypothesis that the target detection system includes parietal and superior frontal cortex while the bottom-up system evoked by salient distractors is more ventral and includes temporoparietal and inferior frontal cortex. We found that presentation of targets was associated with BOLD changes in a distributed anterior and left predominant network that included frontal, temporal, parietal, occipital and limbic cortex as well as thalamic and basal ganglia components. We have documented activation in the medial frontal areas that have been consistently reported in earlier studies, and also in association and limbic regions. For novelty detection, we documented a more posterior and ventral network that included activation of occipital regions and memory related systems in parahippocampal cortices and the right inferior frontal region. Both target and novel stimuli were associated with changes in left thalamus, caudate and cuneus and right parietal precuneus. While all activated regions showed changes conforming to the standard canonical HRF for the novel distractors, this was not the case for targets. Most notable was a negative HRF in the right parietal precuneus, while the same region showed the typical HRF for novels. Biphasic HRFs characterized occipital, thalamic and basal ganglia changes for targets. The association between activation indices and performance encourages further work on characterization of the HRF in regions activated by attentional tasks. While sex differences and age effects were significant, they were subtle in this sample of healthy young adults. However, their presence in this sample with an easy attentional task indicates that such indices could serve to examine individual differences and effects of brain dysfunction.

ACKNOWLEDGMENTS

The authors thank Leif Finkel, PhD, for constructing the visual stimuli, Lee Schroeder for help in design and implementation, and Norman Butler and the staff of the Center for Functional Imaging for help in data acquisition.

REFERENCES

Andersson JL (1997): How to estimate global activity independent of changes in local activity. Neuroimage 6:237–244.

Ardekani BA, Choi SJ, Hossein-Zadeh GA, Porjesz B, Tanabe JL, Lim KO, Bilder R, Helpern JA, Begleiter H (2002): Functional magnetic resonance imaging of brain activity in the visual oddball task. Brain Res Cogn Brain Res 14:347–356.

Bahramali H, Gordon E, Lagopoulos J, Lim CL, Li W, Leslie J, Wright JJ (1999): The effects of age on late components of the ERP and reaction time. Exp Aging Res 26:69–80.

Bledowski C, Prvulovic D, Goebel R, Zanella FE, Linden DE (2004): Attentional systems in target and distractor processing: A combined ERP and fMRI study. Neuroimage 22:530–540.

Boynton GM, Engel SA, Glover GH, Heeger DJ (1996): Linear systems analysis of functional magnetic resonance imaging in human V1. J Neurosci 16:4207–4221.

Buxton RB (2001): The elusive initial dip. Neuroimage 13:953–958.

Chute D, Westall R (1997): PowerLaboratory. Devon, PA: MacLaboratory, Inc.

Clark VP, Fannon S, Lai S, Benson R, Bauer L (2000): Responses to rare visual target and distractor stimuli using event-related fMRI. J Neurophysiol 83:3133–3139.

Corbetta M, Shulman GL (2002): Control of goal-directed and stimulus-driven attention in the brain. Nat Rev Neurosci 3:201–215.

Courchesne E (1978): Changes in P3 waves with event repetition: Long-term effects on scalp distribution and amplitude. Electroencephalgr Clin Neurophysiol 45:754–766.

Courchesne E, Hillyard SA, Galambos R (1975): Stimulus novelty, task relevance and the visual evoked potential in man. Electroencephalogr Clin Neurophysiol 39:131–143.

Coyle S, Gordon E, Howson A, Meares RA (1991): The effects of age on auditory event-related potentials. Exp Aging Res 17:103–111.

Dale AM (1999): Optimal experimental design for event-related fMRI. Hum Brain Mapp 8:109–114.

Dilharreguy B, Jones RA, Moonen CT (2003): Influence of fMRI data sampling on the temporal characterization of the hemodynamic response. Neuroimage 19:1820–1828.

Donchin E (1981): Presidential address, 1980. Surprise!. . .Surprise? Psychophysiol 18:493–513.

Duong TQ, Kim DS, Ugurbil K, Kim SG (2000): Spatiotemporal dynamics of the BOLD fMRI signals: Toward mapping submillimeter cortical columns using the early negative response. Magn Reson Med 44:231–242.

First MB, Spitzer RL, Gibbon M, Williams JBW (1995): Structured Clinical Interview for DSM-IV Axis I Disorders, Non-Patient Edition (SCID-NP). Biometrics Research Department, New York State Psychiatric Institute.

Fjell AM, Walhovd KB (2003): On the topography of P3a and P3b across the adult lifespan–a factor-analytic study using orthogonal procrustes rotation. Brain Topogr 15:153–164.

Ford JM, Gray M, Whitfield SL, Turken AU, Glover G, Faustman WO, Mathalon DH (2004): Acquiring and inhibiting prepotent responses in schizophrenia: Event-related brain potentials and functional magnetic resonance imaging. Arch Gen Psychiatry 61:119–129.

Forman SD, Cohen JD, Fitzgerald M, Eddy WF, Mintun MA, Noll DC (1995): Improved assessment of significant activation in functional magnetic resonance imaging (fMRI): Use of a cluster-size threshold. Magn Reson Med 33:636–647.

Frick KM, Gresack JE (2003): Sex differences in the behavioral response to spatial and object novelty in adult C57BL/6 mice. Behav Neurosci 117:1283–1291.

Friedman D, Kazmerski VA, Cycowicz YM (1998): Effects of aging on the novelty P3 during attend and ignore oddball tasks. Psychophysiol 35:508–520.

Friston KJ, Jezzard P, Turner R (1994a): Analysis of functional MRI time-series. Hum Brain Mapp 1:153–171.

Friston KJ, Worsley KJ, Frackowiak RSJ, Mazziotta JC, Evans AC (1994b): Assessing the significance of focal activations using their spatial extent. Hum Brain Mapp 1:210–220.

Friston KJ, Josephs O, Zarahn E, Holmes AP, Rouquette S, Poline JB (2000): To smooth or not to smooth? Bias and efficiency in fMRI time-series analysis. Neuroimage 12:196–208.

Gehring WJ, Goss B, Coles MGH, Meyer DE, Donchin E (1993): A neural system for error detection and compensation. Psychol Sci 4:385–390.

Goldstein A, Spencer KM, Donchin E (2002): The influence of stimulus deviance and novelty on the P300 and novelty P3. Psychophysiol 39:781–790.

Gur RC, Gur RE, Obrist WD, Hungerbuhler JP, Younkin D, Rosen AD, Skolnick BE, Reivich M (1982): Sex and handedness differences in cerebral blood flow during rest and cognitive activity. Science 217:659–661.

Gur RC, Gur RE, Obrist WD, Skolnick BE, Reivich M (1987): Age and regional cerebral blood flow at rest and during cognitive activity. Arch Gen Psychiatry 44:617–621.

Gur RC, Erwin RJ, Gur RE (1992): Neurobehavioral probes for physiologic neuroimaging studies. Arch Gen Psychiatry 49:409–414.

Gur RC, Ragland JD, Mozley LH, Mozley PD, Smith R, Alavi A, Bilker W, Gur RE (1997): Lateralized changes in regional cerebral blood flow during performance of verbal and facial recognition tasks: Correlations with performance and effort. Brain Cogn 33:388–414.

Gur RC, Alsop D, Glahn D, Petty R, Swanson CL, Maldjian JA, Turetsky BI, Detre JA, Gee J, Gur RE (2000): An fMRI study of sex differences in regional activation to a verbal and a spatial task. Brain Lang 74:157–170.

Hall DA, Goncalves MS, Smith S, Jezzard P, Haggard MP, Kornak J (2002): A method for determining venous contribution to BOLD contrastsensory activation. Magn Res Imaging 20:695–706.

Hirayasu Y, Samura M, Ohta H, Ogura C (2000): Sex effects on rate of change of P300 latency with age. Clin Neurophysiol 111:187–194.

Hoffman LD, Polich J (1999): P300, handedness, and corpus callosal size: Gender, modality, and task. Int J Psychophysiol 31:163–174.

Hori J, Aiba M, He B (2004): Spatio-temporal cortical source imaging of brain electrical activity by means of time-varying parametric projection filter. IEEE Trans Biomed Eng 51:768–777.

Huettel SA, McCarthy G (2001): Regional differences in the refractory period of the hemodynamic response: An event-related fMRI study. Neuroimage 14:967–976.

Huettel SA, McCarthy G (2004): What is odd in the oddball task? Prefrontal cortex is activated by dynamic changes in response strategy. Neuropsychologia 42:379–386.

Hulvershorn J, Bloy L, Gualtieri EE, Leigh JS, Elliott MA (2005): Spatial sensitivity and temporal response of spin echo and gradient echo BOLD contrast at 3 T using peak hemodynamic activation time. Neuroimage 24:216–233.

Jones M, Berwick J, Johnston D, Mayhew J (2001): Concurrent optical imaging spectroscopy and laser-Doppler flowmetry: The relationship between blood flow, oxygenation, and volume in rodent barrel cortex. Neuroimage 13:1002–1015.

Kerns JG, Cohen JD, MacDonald AW III, Cho RY, Stenger VA, Carter CS (2004): Anterior cingulate conflict monitoring and adjustments in control. Science 303:1023–1026.

Kiehl KA, Liddle PF (2003): Reproducibility of the hemodynamic response to auditory oddball stimuli: A six-week test-retest study. Hum Brain Mapp 18:42–52.

Kirino E, Belger A, Goldman-Rakic P, McCarthy G (2000): Prefrontal activation evoked by infrequent target and novel stimuli in a visual target detection task: An event-related functional magnetic resonance imaging study. J Neurosci 20:6612–6618.

Knight RT (1984): Decreased response to novel stimuli after prefrontal lesions in man. Electroencephalgr Clin Neurophysiol 59:9–20.

Knight RT, Nakada T (1998): Cortico-limbic circuits and novelty: A review of EEG and blood flow data. Rev Neurosci 9:57–70.

Knight RT, Scabini D, Woods DL, Clayworth C (1988): The effects of lesions of superior temporal gyrus and inferior parietal lobe on temporal and vertex components of the human AEP. Electroencephalgr Clin Neurophysiol 70:499–509.

Kruggel F, von Cramon DY (1999): Temporal properties of the hemodynamic response in functional MRI. Hum Brain Mapp 8:259–271.

Lancaster JL, Rainey LH, Summerlin JL, Freitas CS, Fox PT (1997): Automated labeling of the human brain: A preliminary report

on the development and evaluation of a forward-transform method. Hum Brain Mapp 5:238–242.

Lee AT, Glover GH, Meyer CH (1995): Discrimination of large venous vessels in time-course spiral blood-oxygen-level-dependent magnetic-resonance functional neuroimaging. Magn Reson Med 33:745–754.

Linden DE, Prvulovic D, Formisano E, Vollinger M, Zanella FE, Goebel R, Dierks T (1999): The functional neuroanatomy of target detection: An fMRI study of visual and auditory oddball tasks. Cereb Cortex 9:815–823.

Liu HL, Pu Y, Nickerson LD, Liu Y, Fox PT, Gao JH (2000): Comparison of the temporal response in perfusion and BOLD-based event-related functional MRI. Magn Reson Med 43:768–772.

Madden DJ, Whiting WL, Provenzale JM, Huettel SA (2004): Age-related changes in neural activity during visual target detection measured by fMRI. Cereb Cortex 14:143–155.

Maeshima S, Okita R, Yamaga H, Ozaki F, Moriwaki H (2003): Relationships between event-related potentials and neuropsychological tests in neurologically healthy adults. J Clin Neurosci 10:60–62.

McCarthy G, Luby M, Gore J, Goldman-Rakic P (1997): Infrequent events transiently activate human prefrontal and parietal cortex as measured by functional MRI. J Neurophysiol 77:1630–1634.

Mesulam MM (1999): Spatial attention and neglect: Parietal, frontal and cingulate contributions to the mental representation and attentional targeting of salient extrapersonal events. Philos Trans R Soc Lond B Biol Sci 354:1325–1346.

Nagy E, Potts GF, Loveland KA (2003): Sex-related ERP differences in deviance detection. Int J Psychophysiol 48:285–292.

Pelizzari CA, Chen GT, Spelbring DR, Weichselbaum RR, Chen CT (1989): Accurate three-dimensional registration of CT, PET, and/or MR images of the brain. J Comput Assist Tomogr 13: 20–26.

Picton TW (1992): The P300 wave of the human event-related potential. J Clin Neurophysiol 9:456–479.

Ragland JD, Turetsky BI, Gur RC, Gunning-Dixon F, Turner T, Schroeder L, Chan R, Gur RE (2002): Working memory for complex figures: An fMRI comparison of letter and fractal N-Back tasks. Neuropsychology 16:370–379.

Robson MD, Dorosz JL, Gore JC (1998): Measurements of the temporal fMRI response of the human auditory cortex to trains of tones. Neuroimage 7:185–198.

Rosen BR, Buckner RL, Dale AM (1998): Event-related functional MRI: Past, present, and future. Proc Natl Acad Sci USA 95:773–780.

Saad ZS, Ropella KM, Cox RW, DeYoe EA (2001): Analysis and use of FMRI response delays. Hum Brain Mapp 13:74–93.

Shaywitz BA, Shaywitz SE, Pugh KR, Constable RT, Skudlarski P, Fulbright RK, Bronen RA, Fletcher JM, Shankweiler DP, Katz L, Gore JC (1995): Sex differences in the functional organization of the brain for language. Nature 373:607–609.

Shmuel A, Yacoub E, Pfeuffer J, Van de Moortele PF, Adriany G, Hu X, Ugurbil K (2002): Sustained negative BOLD, blood flow and oxygen consumption response and its coupling to the positive response in the human brain. Neuron 36:1195–1210.

Spencer KM, Dien J, Donchin E (2001): Spatiotemporal analysis of the late ERP responses to deviant stimuli. Psychophysiology 38:343–358.

Squires NK, Squires KC, Hillyard SA (1975): Two varieties of long-latency positive waves evoked by unpredictable auditory stimuli in man. Electroencephalgr Clin Neurophysiol 38:387–401.

Sutton S, Braren M, Zubin J, John ER (1965): Evoked-potential correlates of stimulus uncertainty. Science 150:1187–1188.

Talairach J, Tournoux P (1988): Co-planar stereotaxic atlas of the human brain: 3-Dimensional proportional system: An approach to cerebral imaging. New York: Thieme Medical Publishers.

Vanzetta I, Grinvald A (2001): Evidence and lack of evidence for the initial dip in the anesthetized rat: Implications for human functional brain imaging. Neuroimage 13:959–967.

van Zijl PC, Ulug AM, Eleff SM, Ulatowski JA, Traystman RJ, Oja JM, Kauppinen RA (1998): Quantitative assessment of blood flow, blood volume and blood oxygenation effects in functional magnetic resonance imaging. Nat Med 4:159–167.

Wang J, Alsop DC, Song HK, Maldjian JA, Tang K, Salvucci AE, Detre JA (2003): Arterial transit time imaging with flow encoding arterial spin tagging (FEAST). Magn Reson Med 50:599–607.

Williams LM, Brammer MJ, Skerrett D, Lagopolous J, Rennie C, Kozek K, Olivieri G, Peduto T, Gordon E (2000): The neural correlates of orienting: An integration of fMRI and skin conductance orienting. Neuroreport 11:3011–3015.

Woods RP, Mazziota JC, Cherry SR (1993):Automated image registration. In:Uemura K, Lassen NA,Jones T,Kanno I, editors. Quantification of Brain Function: Tracer Kinetics and Image Analysis in Brain PET. Amsterdam: Elsevier. pp 391–398.

Zink CF, Pagnoni G, Martin ME, Dhamala M, Berns GS (2003): Human striatal response to salient nonrewarding stimuli. J Neurosci 23:8092–8097.